

# Exercise reduces intramuscular stress and counteracts muscle weakness in mice with breast cancer

Theresa Mader<sup>1</sup>, Thomas Chaillou<sup>1,2</sup>, Estela Santos Alves<sup>1</sup>, Baptiste Jude<sup>1</sup>, Arthur J. Cheng<sup>1,3</sup>, Ellinor Kenne<sup>1</sup>, Sara Mijwel<sup>1,4</sup>, Ewa Kurzejamska<sup>5</sup>, Clara Theresa Vincent<sup>5,6</sup>, Helene Rundqvist<sup>7</sup> & Johanna T. Lanner<sup>1\*</sup> 

<sup>1</sup>Department of Physiology and Pharmacology, Molecular Muscle Physiology and Pathophysiology, Karolinska Institutet, Biomedicum, Stockholm, Sweden; <sup>2</sup>School of Health Sciences, Örebro University, Örebro, Sweden; <sup>3</sup>Muscle Health Research Centre, School of Kinesiology and Health Science, Faculty of Health Toronto, York University, Toronto, Ontario, Canada; <sup>4</sup>Department of Neurobiology, Care Sciences and Society, Karolinska Institutet, Stockholm, Sweden; <sup>5</sup>Department of Immunology, Genetics and Pathology, Uppsala University, Uppsala, Sweden; <sup>6</sup>Department of Microbiology, NYU Grossman School of Medicine, New York, NY, USA; <sup>7</sup>Department of Laboratory Medicine, Clinical Physiology, Karolinska Institutet, Stockholm, Sweden

## Abstract

**Background** Patients with breast cancer exhibit muscle weakness, which is associated with increased mortality risk and reduced quality of life. Muscle weakness is experienced even in the absence of loss of muscle mass in breast cancer patients, indicating intrinsic muscle dysfunction. Physical activity is correlated with reduced cancer mortality and disease recurrence. However, the molecular processes underlying breast cancer-induced muscle weakness and the beneficial effect of exercise are largely unknown.

**Methods** Eight-week-old breast cancer (MMTV-PyMT, PyMT) and control (WT) mice had access to active or inactive in-cage voluntary running wheels for 4 weeks. Mice were also subjected to a treadmill test. Muscle force was measured *ex vivo*. Tumour markers were determined with immunohistochemistry. Mitochondrial biogenesis and function were assessed with transcriptional analyses of PGC-1 $\alpha$ , the electron transport chain (ETC) and antioxidants superoxide dismutase (Sod) and catalase (Cat), combined with activity measurements of SOD, citrate synthase (CS) and  $\beta$ -hydroxyacyl-CoA-dehydrogenase ( $\beta$ HAD). Serum and intramuscular stress levels were evaluated by enzymatic assays, immunoblotting, and transcriptional analyses of, for example, tumour necrosis factor- $\alpha$  (TNF- $\alpha$ ) and p38 mitogen-activated protein kinase (MAPK) signalling.

**Results** PyMT mice endured shorter time and distance during the treadmill test ( $\sim$ 30%,  $P < 0.05$ ) and *ex vivo* force measurements revealed  $\sim$ 25% weaker slow-twitch soleus muscle ( $P < 0.001$ ). This was independent of cancer-induced alteration of muscle size or fibre type. Inflammatory stressors in serum and muscle, including TNF- $\alpha$  and p38 MAPK, were higher in PyMT than in WT mice ( $P < 0.05$ ). Cancer-induced decreases in ETC ( $P < 0.05$ ,  $P < 0.01$ ) and antioxidant gene expression were observed ( $P < 0.05$ ). The exercise intervention counteracted the cancer-induced muscle weakness and was accompanied by a less aggressive, differentiated tumour phenotype, determined by increased CK8 and reduced CK14 expression ( $P < 0.05$ ). In PyMT mice, the exercise intervention led to higher CS activity ( $P = 0.23$ ), enhanced  $\beta$ -HAD and SOD activities ( $P < 0.05$ ), and reduced levels of intramuscular stressors together with a normalization of the expression signature of TNF $\alpha$ -targets and ETC genes ( $P < 0.05$ ,  $P < 0.01$ ). At the same time, the exercise-induced PGC-1 $\alpha$  expression, and CS and  $\beta$ -HAD activity was blunted in muscle from the PyMT mice as compared with WT mice, indicative that breast cancer interfere with transcriptional programming of mitochondria and that the molecular adaptation to exercise differs between healthy mice and those afflicted by disease.

**Conclusions** Four-week voluntary wheel running counteracted muscle weakness in PyMT mice which was accompanied by reduced intrinsic stress and improved mitochondrial and antioxidant profiles and activities that aligned with muscles of healthy mice.

**Keywords** Muscle weakness; Breast cancer; Stress; Mitochondria

Received: 9 June 2021; Revised: 12 January 2022; Accepted: 18 January 2022

\*Correspondence to: Johanna T. Lanner, Department of Physiology and Pharmacology, Molecular Muscle Physiology and Pathophysiology, Karolinska Institutet, Biomedicum, Solnavägen 9, SE-17177 Stockholm. Phone: +46720058348, Email: johanna.lanner@ki.se

## Introduction

Breast cancer is the most commonly diagnosed cancer type in women with around two million new cases per year worldwide.<sup>1</sup> Muscle weakness in cancer patients has traditionally been attributed to a decrease in muscle mass (i.e. atrophy); however, breast cancer patients exhibit a low prevalence of cachexia.<sup>2,3</sup> Nevertheless, loss in muscle strength and reduced physical fitness are already experienced in weight-stable, non-cachectic patients in the early stages of breast cancer development.<sup>4,5</sup> A marked reduction in muscle force by 25% has been presented in the lower extremities of breast cancer patients before and after anticancer treatments.<sup>5</sup> Overall, muscle weakness is associated with reduced quality of life and higher mortality risk in cancer, including breast cancer,<sup>6</sup> highlighting the critical role of muscle function for physical health.

Pre-diagnosis and post-diagnosis recreational physical activity offers a significant risk reduction for breast cancer-related death.<sup>7–9</sup> For example, post-diagnosis physical activity of moderate intensity, equivalent of walking 3 to 5 h per week or endurance exercise for 150 min/week, reduces cancer death and breast cancer recurrence by ~30–40% as compared with inactive individuals.<sup>7–10</sup> This non-anabolic physical activity does not build muscle mass but may instead preserve muscle fibre area and mitochondrial oxidative capacity, thus improving the quality of the skeletal muscle. Moreover, a comparison of skeletal muscle biopsies from breast cancer patients under chemotherapy treatment, subjected to different exercise regimens showed that the exercise interventions prevented a reduction in muscle fibre cross-sectional area and mitochondrial capacity which was observed in the usual care group.<sup>11</sup>

Still, little is known about the molecular aspects of muscle weakness and the beneficial effect of exercise in breast cancer, especially without interference of chemotherapeutic drugs, which is not possible in a clinical setting. We used *in vivo* endurance tests, *ex vivo* functional force measurements of single fibres and whole muscle, combined with morphological and molecular analyses to evaluate muscle function and exercise-induced effects during progressive breast cancer development. The breast cancer mouse model PyMT (MMTV-PyMT, FVB background) resembling morphological and molecularly the human tumour progression was used.<sup>12</sup> Mice, 8 weeks old, without any anti-tumour treatment underwent 4 weeks of voluntary in-cage wheel running as exercise intervention, to elucidate the exercise-induced effects of skeletal muscle function in mice afflicted by breast cancer.

## Materials and methods

### Study approval

All animal experiments complied with the Swedish Animal Welfare Act, the Swedish Welfare ordinance, and regulations of the Swedish authorities (N19-15, 3067-2018, 6847-2020).

### Animals

Female mice (FVB/N-MMTV-PyMT) with polyoma virus middle T oncoprotein (PyMT) under the control of the mice mammary tumour virus (MMTV) promoter, and their wildtype (WT) littermates (WT, FVB/NRj background) were used.<sup>12</sup> Mice were housed at the local animal facility with a 12 h light/dark cycle and provided standard chow and water *ad libitum*. Tumour dimensions were measured with standard callipers. All mice were 8 weeks of age at the start of all experiments and sacrificed at 12 weeks of age.

### Treadmill running

A six-lane treadmill was used. Individual mice were separated by partitions. After 4 days of acclimatization, the exhaustion test was performed with a 10% inclination and speed increment from 6 m/min to maximal 33 m/min (kept till exhaustion) by 3 m/min every 3 min. Exhaustion was determined by the mice withstanding three manual pushes, in combination of a behavioural assessment when placed into a new environment.

### Voluntary wheel running

Mice were housed individually and given free access to either a counting (active) or blocked (inactive) low-profile wireless running wheel for 4 weeks (ENV-047 or ENV-044-02, Med Associates Inc.).

### Immunofluorescence analysis and FCSA (muscle sections)

Serial transverse sections of fresh soleus muscles were used for as previously described.<sup>13</sup> Sections were incubated with primary antibodies against myosin heavy chain (MHC) isoforms (MHC1, BA-D5; MHC2a, SC.71. Hybridoma Bank) and thereafter with secondary antibodies (IgG2b Alexa Flour

350, A21140; IgG1 Alexa Flour 488, A21121, Invitrogen). Sections were incubated with Wheat Germ Agglutinin conjugated with TX-Red (W21405, Invitrogen) to image the sarcolemma. Fibre type distribution was determined based on fibres expressing MHC1 (type-1 fibres), MHC2a (type-2a fibres), and unstained fibres (type 2x/2b fibres). Fibre-type, FCSA and FCSA distribution were analysed from  $251 \pm 23$  fibres per muscle on average.

### *Immunohistochemical analysis (tumour sections)*

Sections of 10  $\mu\text{m}$  tumour tissue were imaged for CK8 (ab59400) and CK14 (ab181595) as previously described.<sup>14</sup> The images were quantified with Image J using 16–20 visual fields/tumour. Equal colour threshold was used for all conditions compared.

### *Ex vivo force measurement*

Force measurements of soleus and extensor digitorum longus (EDL) were performed as previously described.<sup>15</sup> Electrically stimulated force production was expressed as absolute force (mN) and as specific force ( $\text{kN}/\text{m}^2$ ). To determine the specific force, that is, force normalized to muscle size, absolute force was divided with muscle cross-sectional area (CSA) which was calculated by dividing the muscle mass by the muscle length and muscle density ( $1.06 \text{ g}/\text{cm}^3$ ). After the experiment, the tendons were cut to determine muscle mass.

### *Single soleus fibre experiments*

Isolated, intact single muscle fibres were mechanically dissected from slow-twitch soleus muscles of PyMT and control littermate mice and simultaneous quantification of force and  $[\text{Ca}^{2+}]_i$  in living single fibres with a completely intact intracellular milieu were performed as previously described in detail.<sup>16</sup> Some fibres were exposed to caffeine (5 mM), a potent RyR1 agonist,<sup>17</sup> and stimulated at 120 Hz.

### *Immunoblots (western blots)*

Immunoblots were performed as previously described.<sup>13</sup> Homogenized tibialis anterior (TA) or soleus (20  $\mu\text{g}$  per well) were separated and transferred to PVDF membranes (Millipore). Membranes were incubated with primary antibodies: phospho-p38 MAPK (#9211, Thr180/Tyr182, Cell Signaling), p38 MAPK (#9212, Cell Signaling), RyR1 (#ab2868), CSQ1,2 (#ab3516), and DHPR (#ab2864) and thereafter with infrared-labelled secondary antibodies (IRDye 680, IRDye 800, LI-COR Biosciences). Detection and analyses were performed with the LI-COR imaging system and normalized to to-

tal protein, which was determined by Ponceau S or Coomassie staining.

### *Citrate synthase and $\beta$ -hydroxyacyl-CoA dehydrogenase activities activity assays*

Soleus muscles were homogenized in ice-cold homogenization buffer at pH 7.5 consisting of (mM):  $\text{KH}_2\text{PO}_4$ , 50; EDTA, 1; and 0.05% Triton X-100. The homogenate was centrifuged at 1400  $g$  for 1 min at  $4^\circ\text{C}$ . The supernatant was used to analyse citrate synthase (CS) and  $\beta$ -hydroxyacyl-CoA dehydrogenase ( $\beta$ -HAD) activities using standard spectrophotometric techniques.<sup>18</sup> Activities were adjusted for protein concentration.

### *TNF- $\alpha$ levels*

A total of 5  $\mu\text{L}$  serum or 5  $\mu\text{g}$  soleus muscle protein lysates were used to quantify TNF- $\alpha$  levels using an ELISA kit according to the manufacturer's instructions (ThermoFisher).

### *SOD activity assay*

Gastrocnemius muscles (10 mg) were pulverized and homogenized in ice cold 0.1 M Tris/HCl, pH 7.4 buffer containing 0.5% Triton X-100, 5 mM  $\beta$ -ME, 0.1 mg/mL PMSF. SOD activity was determined with the colorimetric kit (#ab64354) according to the manufacturer's instructions. Values were normalized to mg of muscle weight.

### *Gene expression analysis*

Gene expression of gastrocnemius muscle was performed as previously described.<sup>13</sup> Analysis of gene expression was performed with the  $\Delta\Delta\text{Ct}$  method, and gene expression was normalized to ribosomal protein lateral stalk subunit P0 (RPLP0) mRNA levels. Gene expression analyses are expressed as mRNA levels relative to WT. Primer sequences used for gene expression analysis can be found in the Supporting Information, Table S1.

### *Statistics*

Data are presented as mean  $\pm$  SEM or as box-plot and whiskers-plot with the median of the distribution indicated as horizontal line, the boundaries indicate the medians of the first and third quartiles, and the error bars extend to the extremes of the observation. Two groups were analysed by two-tailed unpaired Student's  $t$ -test. Multiple comparisons were analysed by analysis of variance (ANOVA).  $P$  values

<0.05 were considered significant (\* $P < 0.05$ ; \*\* $P < 0.01$ ; \*\*\* $P < 0.001$ ). All statistical analysis was carried out with Prism 7.0 (GraphPad).

## Results

### *PyMT mice exhibit reduced physical performance and muscle weakness*

To test their overall physical performance, PyMT mice and WT mice ran till exhaustion on a treadmill at 12 weeks of age. PyMT mice ran ~20% shorter and covered ~30% less distance on the treadmill as compared with control WT mice (Figure 1A and 1B). In addition to mobility hindrance due to tumour mass, reduced physical performance may also be the result of altered skeletal muscle function, including muscle size, morphological changes, and/or intrinsic muscle dysfunction. Here, the muscle mass of hind limb muscles (TA; EDL; soleus) was unchanged between PyMT and WT mice (Figure 1C). *Ex vivo* isometric force measurements showed a drastic reduction in absolute and specific force by ~22% of PyMT slow-twitch soleus muscle as compared with WT mice (Figure 1D and 1E). No difference in force production was observed in fast-twitch EDL muscle (Figure S1A,B), and thus, focus was pointed towards slow-twitch (soleus) and mixed muscle fibre types (TA and gastrocnemius). No difference in size or distribution of muscle fibre cross-sectional area (FCSA) or fibre type composition (MHC isoforms) was observed of soleus muscle from PyMT and WT (Figure 1F–1I). Moreover, no difference in expression levels of proteins essential for the excitation–contraction coupling [the  $\text{Ca}^{2+}$  release channel ryanodine receptor 1 (RyR1),  $\text{Ca}^{2+}$  buffering protein calsequestrin (CSQ) 1 and 2, or the voltage-gated dihydropyridine receptor (DHPR,  $\text{Cav}_{1.1}$ )] was observed between soleus muscle from WT and PyMT mice (Figure S1C, D). This shows that the observed muscle weakness was not a result of reduced muscle size or altered morphology, but rather due to intrinsic impairment of the muscular function as evident in Figure 1E (specific force,  $\text{kN/m}^2$ ). Further simultaneous measurements of cytosolic  $\text{Ca}^{2+}$  concentrations ( $[\text{Ca}^{2+}]_i$ ) and force in single intact mechanically dissected soleus fibres showed that the muscle weakness (Figure 1K and 1L) was not associated with a difference in basal  $[\text{Ca}^{2+}]_i$  between groups ( $0.054 \pm 0.004 \mu\text{M}$  vs.  $0.055 \pm 0.02 \mu\text{M}$ ,  $P = 0.96$ ), but tetanic  $[\text{Ca}^{2+}]_i$  was modestly reduced in soleus fibres from PyMT mice (Figure 1J and 1K). Force– $[\text{Ca}^{2+}]_i$  curves were constructed by fitting the mean data points to the following equation:  $P = P_{\text{max}}[\text{Ca}^{2+}]_i^N / (\text{Ca}_{50}^N + [\text{Ca}^{2+}]_i^N)$ , where  $P$  is the measured force,  $P_{\text{max}}$  the predicted maximum force at saturating  $[\text{Ca}^{2+}]_i$ ,  $\text{Ca}_{50}$  the  $[\text{Ca}^{2+}]_i$  at 50%  $P_{\text{max}}$ , and  $N$  describes the steepness of the force– $[\text{Ca}^{2+}]_i$  relationship.  $P_{\text{max}}$  was lower (382 vs. 263  $\text{kN/m}^2$ ,  $P = 0.02$ ) in PyMT fibres, whereas

no difference in  $\text{Ca}_{50}$  (0.56 vs.  $0.47 \mu\text{M}$ ,  $P = 0.44$ ) or in the steepness of the relationships ( $N$  4.83 vs. 5.95,  $P = 0.51$ ) was observed between the two groups (Figure 1L). This implies that the decreased force in PyMT fibres is the result of myofibrillar impairment rather than a problem linked to reduced  $\text{Ca}^{2+}$  sensitivity. Moreover, fibres were exposed to caffeine (5 mM), a potent RyR1 agonist<sup>17</sup> to assess whether an increased  $[\text{Ca}^{2+}]_i$  could counteract the weakness. A tetanic stimulation (120 Hz) in the presence of caffeine releases virtually all  $\text{Ca}^{2+}$  stored in the sarcoplasmic reticulum and maximally activates the contractile machinery.<sup>19</sup> Caffeine had a large effect on  $[\text{Ca}^{2+}]_i$ , but no difference was observed between WT and PyMT soleus fibres (Figure 1M). The increased tetanic  $[\text{Ca}^{2+}]_i$  with caffeine had no notable effect on force production and hence could not counteract the muscle weakness in PyMT mice (Figure 1N). That the force was not further enhanced in WT can be explained by tetanic force at 120 Hz being close to maximal already before caffeine application. This shows that an increased tetanic  $[\text{Ca}^{2+}]_i$  in PyMT fibres was not capable of counteracting the muscle weakness, emphasizing that the muscle weakness is the results of intrinsic contractile dysfunction.

### *Voluntary running counteracts cancer-induced muscle weakness*

Eight-week-old PyMT and WT mice had individually *ad libitum* access to running wheels for 4 weeks. PyMT and WT mice spent approximately the same amount of time and ran similar distances on the wheel (Figure 2A and 2B). The voluntary wheel running did not alter the tumour volume (Figure 2C) but developed a more favourable molecular profile of the tumour<sup>14</sup> with the luminal epithelial cell marker cytokeratin (CK) 8 slightly increased and the invasive basal marker CK14 decreased with exercise (Figure 2D and 2E). In the performed treadmill exhaustion run, both groups showed improvements in time spent running and meters covered after exercise (active wheels) as compared with non-exercised mice (inactive wheels) (Figure 2F and 2G). The magnitude of improvement (Figure 2F and 2G) was greater in WT than in PyMT mice, showing that the breast cancer attenuates the response to whole body physical exercise performance. To exclude mammary tumours interference on the extremity's mobility in the treadmill test and to specifically address skeletal muscle and contractile function, skeletal muscles were excised and force was measured *ex vivo*. No exercise-induced changes in muscle mass was observed (Figure 2H), but *ex vivo* force measurements showed that the exercise remarkably counteracted cancer-induced muscle weakness in slow-twitch soleus muscle of PyMT mice (Figure 2I and 2J). Thus, without any antitumor treatment, the exercise recovered the intrinsic capacity of the muscle to generate force in mice with breast cancer.

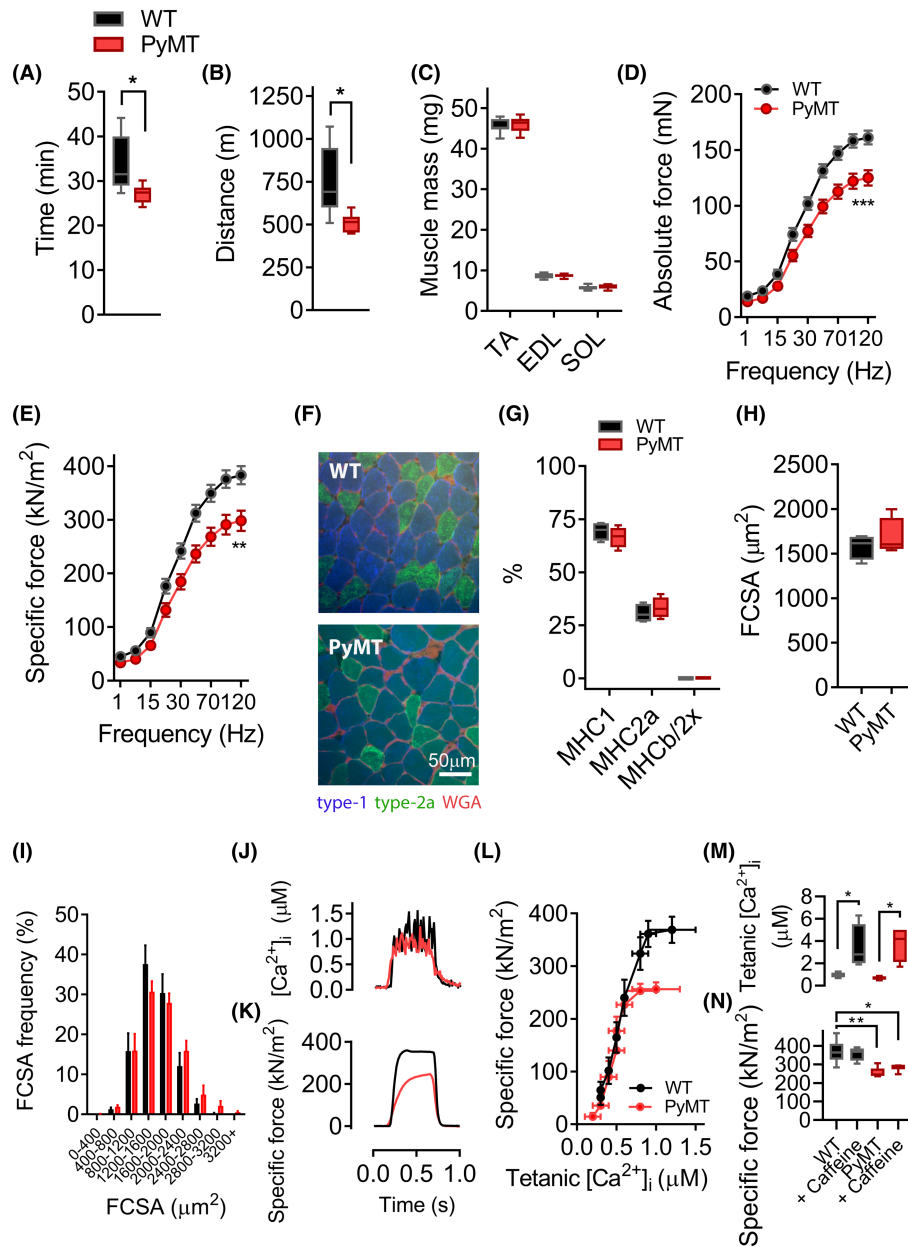


**Figure 1** Reduced exercise performance and muscle weakness in PyMT mice. (A) Time (min) and (B) distance (meter) endured by PyMT and WT mice during a treadmill exhaustion run test. (C) Muscle mass (mg) of tibialis anterior (TA), extensor digitorum longus (EDL) and soleus from PyMT and FVB (WT) mice. (D, E) *Ex vivo* absolute force (D, mN) and specific force (E, kN/m<sup>2</sup>) production of soleus muscle from PyMT and WT mice. The force-frequency relationship was determined at 1, 10, 15, 20, 30, 50, 70, 100, and 120 Hz (1000 ms tetanic duration). (F) Representative images of cross-sectional muscle sections of soleus muscle. Fibre type distribution visualized by fluorescent imaging (20×); myosin heavy chain (MHC) 1 (type-1 fibres, blue), MHC2a (type-2a, green). Wheat germ agglutinin (WGA, red) binds to glycoproteins of the cell membrane and used to stain skeletal sarcolemma to determine cross sectional area. (G) Distribution of MHC isoforms, (H) fibre cross-sectional area (FCSA, μm<sup>2</sup>) and distribution of FCSA area (I, %) of soleus muscle from PyMT and WT mice. (J–N) Specific force and calcium measurements in single soleus fibres. Original records of intracellular (tetanic) Ca<sup>2+</sup> (J, [Ca<sup>2+</sup>]<sub>i</sub>, μM) and specific force (K, kN/m<sup>2</sup>) determined at 120 Hz stimulation frequency (500 ms train duration). (L) Force-Ca<sup>2+</sup> relationship at 15 to 150 Hz stimulation frequencies. (M, N) Caffeine exposure on single muscle fibres at 120 Hz. Intracellular Ca<sup>2+</sup> (M, μM) and specific force (N, kN/m<sup>2</sup>) with and without caffeine (5 mM, 2 min exposure) in PyMT and WT soleus fibres. (A, B, n = 6 per group; C, n = 8–10 per group; D, E, n = 13–18 per group; F, I n = 5–6 per group with 251 ± 23 fibres per muscle analysed on average; L, n = 4–6 per group; M, N, n = 4 per group). D, E, I, and L are presented as mean ± SEM; other average data are presented as box-plot and whiskers-plot, median of the distribution is indicated as horizontal line, the boundaries indicate the medians of the first and third quartiles, and the error bars extend to the extremes of the observation. \*P < 0.05, \*\*P < 0.01, \*\*\*P < 0.001.

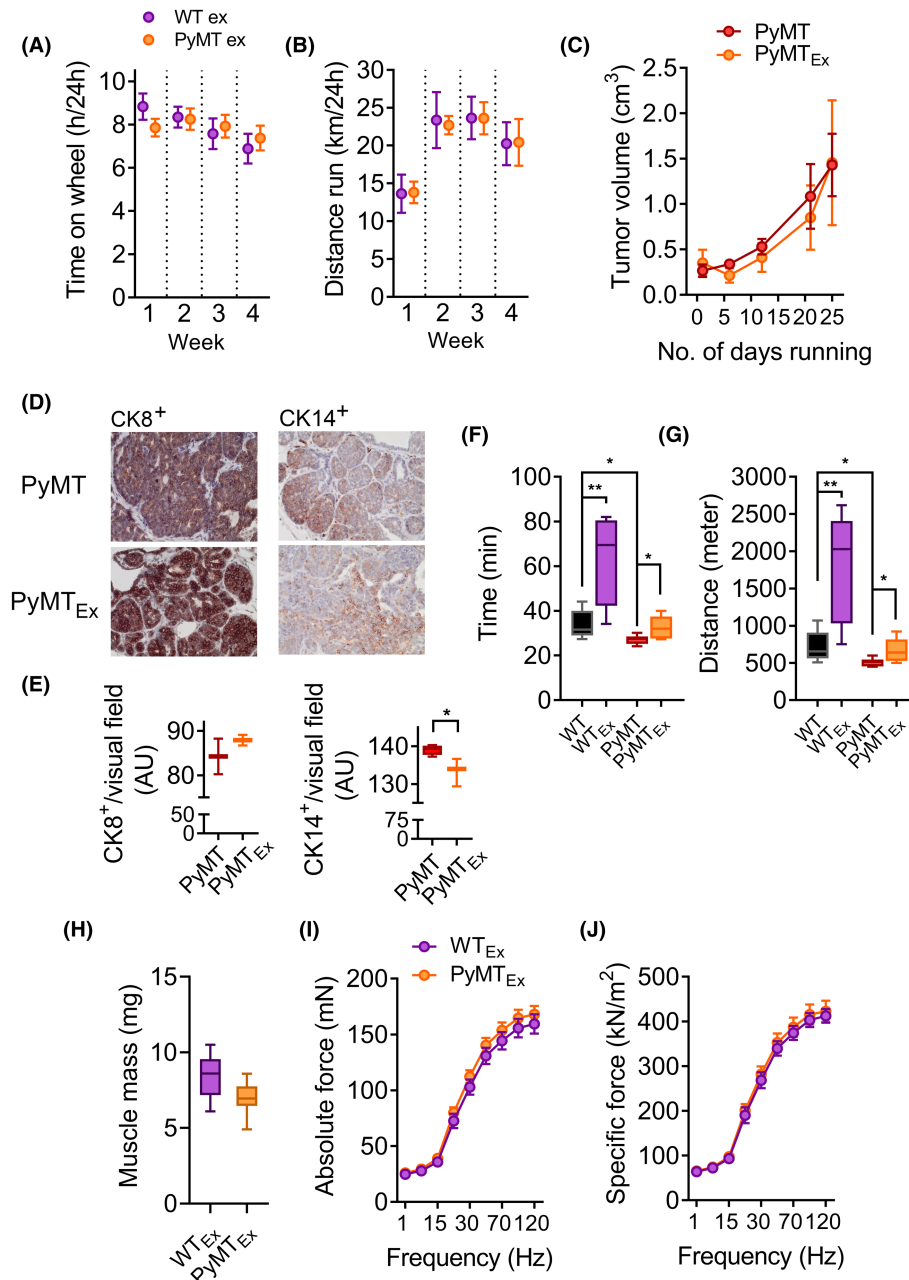


**Figure 2** Voluntary running counteracts muscle weakness. Time (A, h/24 h) and distance (B, km/24 h) mice ran per 24 h per week on the in-cage voluntary running wheels. (C) Average tumour volume in cm<sup>3</sup> measured from start of the exercise intervention at 8 weeks of age and weekly over 4 weeks. Representative histochemical images (D) and quantification (E) of tumours stained for cytokeratin (CK) 8 and CK14 from PyMT mice at 12 weeks of age. Time (F, min) and distance (G, meter) covered running on the treadmill exhaustion test of mice that had access to inactive (WT, PyMT) or active (WT<sub>Ex</sub>, PyMT<sub>Ex</sub>) voluntary in-cage running wheels for 4 weeks. (H) Muscle mass of exercising PyMT and WT mice after 4 weeks of voluntary in-cage running (WT<sub>Ex</sub>, PyMT<sub>Ex</sub>). (I, J) *Ex vivo* force production of soleus muscle from PyMT and WT mice. *Ex vivo* absolute force (I, mN) and specific force (J, kN/m<sup>2</sup>) production of soleus muscle from PyMT and WT mice after 4 weeks of in-cage voluntary running (WT<sub>Ex</sub>, PyMT<sub>Ex</sub>). The force-frequency relationship was determined at 1, 10, 15, 20, 30, 50, 70, 100, and 120 Hz (1000 ms tetanic duration). (A–C and F, G, *n* = 6–10 per group; D, E, *n* = 4 per group with 16–20 visual areas analysed per individual; H–J *n* = 8–12 per group). A–C and I, J are presented as mean ± SEM, other average data are presented as box-plot and whiskers-plot, median of the distribution is indicated as horizontal line, the boundaries indicate the medians of the first and third quartiles and the error bars extend to the extremes of the observation. \**P* < 0.05, \*\**P* < 0.01.

### Altered mitochondrial expression and activity in skeletal muscle of PyMT mice

Reduced mitochondrial function and mitochondrial damage is linked to reduced muscle function and muscle weakness.<sup>13,20,21</sup> Moreover, recent transcriptomics and proteomics analyses showed that mitochondrial ETC genes and proteins were lower in skeletal muscle from breast cancer patients than healthy controls.<sup>22</sup> Here, 8 out of 12 mitochondrial genes representative of mitochondrial complexes I-IV (CI-IV) and the ATP synthase (ATPase) were lower in non-exercised gastrocnemius muscle of PyMT than in WT mice (Figure 3A–3E). The exercise intervention normalized the gene expression of included mitochondrial genes (CII-IV and ATPase) (Figure 3A–3E). Mitochondrial complexes I–IV activities in gastrocnemius muscle of PyMT and WT mice (Figure S1E–S1H) displayed the same pattern as the gene expression profiles (mRNA levels, Figure 3A–3E), that is, non-exercised muscle displayed lower activities in PyMT than WT mice and running exercise resulted in increased activity of mitochondrial ETC complexes (Figure S1E–S1H). The difference in activities was less distinct than in gene expression, exemplifying that transcriptional changes may not directly be transferrable into metabolic adaptations and could also reflect that the analyses were performed in muscles consisting of different fibre types. CS is an integral enzyme in the tricarboxylic acid cycle and used as a marker of mitochondrial content, and  $\beta$ -HAD is a key enzyme in fatty acid oxidation.<sup>23</sup> Enzyme activities (i.e. in non-exercised muscle) of CS and  $\beta$ -HAD appeared lower in soleus muscle from PyMT than WT mice ( $CS_{WT}$ :  $6.2 \pm 0.2$  vs.  $CS_{PyMT}$ :  $5.7 \pm 0.2$ ,  $P = 0.21$ , nmol/mg protein/min,  $n = 6$ .  $\beta$ -HAD- $_{WT}$ :  $0.60 \pm 0.04$  vs.  $\beta$ -HAD- $_{PyMT}$ :  $0.44 \pm 0.03$ ,  $P < 0.05$ , nmol/mg protein/min,  $n = 6$ ) (Figure 3F and 3G). The exercise enhanced the CS and  $\beta$ -HAD activity (Figure 3F and 3G). The magnitude of improvement in treadmill running (Figure 2F and 2G) and mitochondrial enzyme activities (Figure 3F and 3G) was greater in WT than in PyMT mice after the exercise, indicating that the cancer itself attenuates the response to physical exercise in PyMT mice. Nevertheless, the mitochondrial ETC transcriptional profiles and enzyme activities were improved in PyMT mice after the exercise, which likely contributes to the preserved muscle function observed with the exercise intervention.

### Reduced intramuscular stress response in PyMT mice after exercise intervention

Tumour necrosis factor  $\alpha$  (TNF- $\alpha$ ) is a pro-inflammatory cytokine which expression is generally elevated in breast cancer and shown to correlate with higher malignancy grade and generally poor prognosis for the patient.<sup>24</sup> TNF- $\alpha$  signalling has been shown to promote mitochondrial dysfunction and intrinsic muscle weakness by depressing specific force of muscle

fibres.<sup>25,26</sup> Skeletal muscle-specific inhibition of the TNF- $\alpha$  target inhibitor of  $\kappa$ B- $\alpha$  (*I $\kappa$ B- $\alpha$* ) and nuclear factor- $\kappa$ B1 (*NF $\kappa$ B1*) has been shown to protect against cytokine-induced muscle weakness.<sup>27</sup> Thus, the muscle weakness and the altered mitochondrial expression and activity could stem from an enhanced stress response with elevated TNF- $\alpha$  levels originating from the tumour development in the PyMT mice.

TNF- $\alpha$  serum levels were higher in non-exercising PyMT than WT mice, demonstrating a tumour-induced stress response (Figure 4A). The exercise lowered the serum TNF- $\alpha$  level in PyMT mice (Figure 4A) and a similar pattern was observed in a serum cytokine antibody array (Figure S2A). Intramuscular soleus TNF- $\alpha$  levels were also higher in non-exercising PyMT than in WT mice. The exercise drastically reduced the intramuscular TNF- $\alpha$  levels in PyMT mice (Figure 4B), as well as the expression of several TNF- $\alpha$  target genes; TNF receptor-associated factor 2 (*Traf2*) (Figure 4C), *I $\kappa$ B- $\alpha$*  (Figure 4D), ankyrin repeat domain 1 (*Ank1*) (Figure 4E) and *NF $\kappa$ B1* (Figure 4F), but not *NF $\kappa$ B2* (Figure 4G). Moreover, the phosphorylated active form (Thr180/Tyr181) of p38 mitogen-activated protein kinase (MAPK) that responds to cytokines and cellular stress was higher in soleus muscle from non-exercised PyMT than WT mice (Figure 4H and 4I). The exercise intervention decreased the stress response of PyMT mice to levels comparable with WT mice (Figure 4H and 4I). Thus, the exercise intervention with 4 weeks of in-cage running was able to efficiently reduce the systemic and intramuscular stress response in mice with breast cancer.

Pro-inflammatory cytokines as TNF- $\alpha$  can also induce production of reactive oxygen species (ROS). To protect the muscle from ROS and oxidative damage, skeletal muscle are equipped with oxidative scavengers (antioxidants). Superoxide dismutase (*Sod*; isoform 1 localized in the cytosol, and 2 in the mitochondria) and catalase (*Cat*) are two essential antioxidants; where *Sod* scavenges superoxide to hydrogen peroxide which is further metabolized to water by catalase.<sup>28</sup> As observed for ETC and ATPase genes, the exercise intervention reversed *Sod1*, *Sod2* and *Cat* gene expression in PyMT levels comparable with non-exercised WT mice. (Figure 4J and 4K). SOD activity (*SOD1* and *SOD2*) (Figure 4M) showed a similar pattern as the gene expression data (Figure 4J–4L) with the exercise boosting the SOD activity in muscle of PyMT mice. The enhanced antioxidant defence could contribute to improved capacity to neutralize ROS and hence lowered intramuscular oxidative stress. No global change in carbonylation levels (OxyBlot), as oxidative stress biomarker, were observed in TA muscle between the two groups with or without exercise intervention (Figure S2B and S2C). This was expected, tumour-induced oxidative stress in peripheral muscle tissue is likely low grade and continuous, and therefore not necessarily detected using whole muscle extracts. In contrast, tumour tissue from PyMT exhibited higher carbonylation levels than WT mice and the exercise had no evident effect on carbonylation levels (Supplemental Fig, S2D–E).

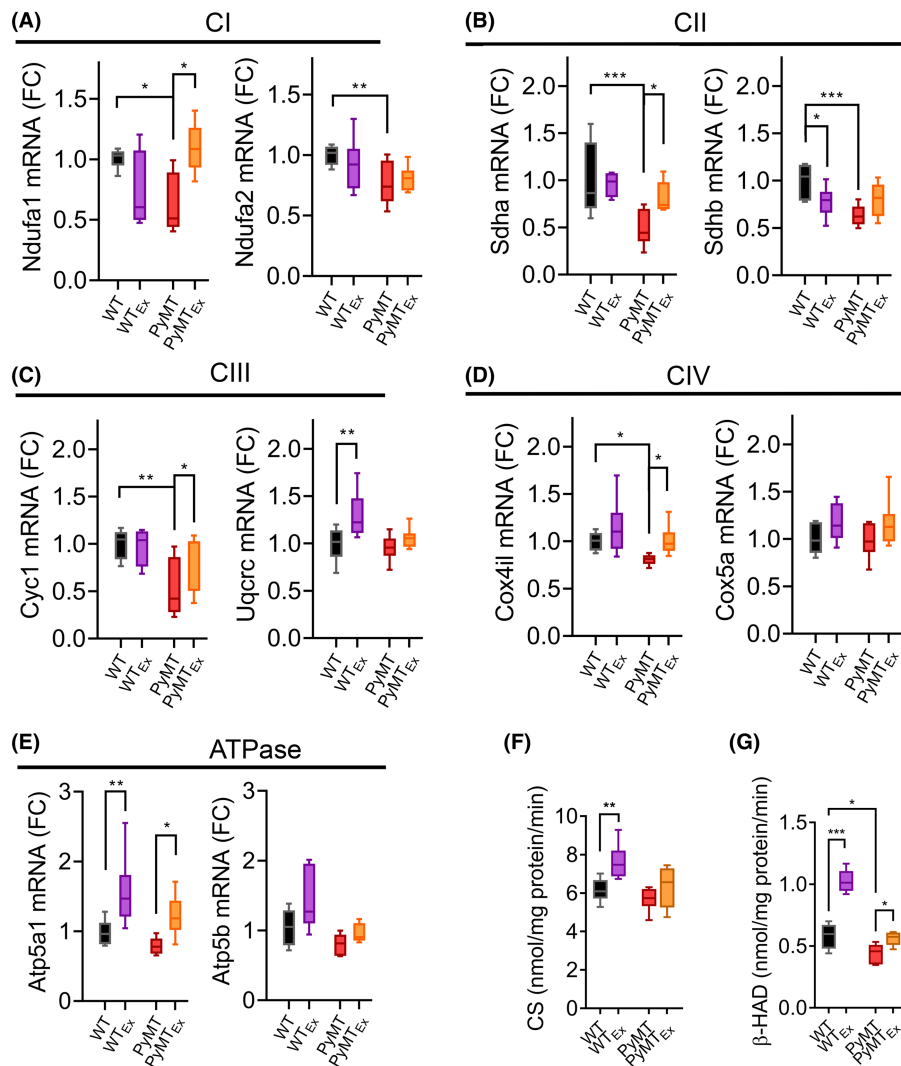


**Figure 3** Running exercise reverses mitochondrial gene expression and activity in PyMT mice. mRNA expression of ETC genes in mitochondria from soleus muscle of WT and PyMT mice after 4 weeks access to inactive (WT, PyMT) or active (WT<sub>Ex</sub>, PyMT<sub>Ex</sub>) in-cage running wheels. (A) Complex (C) I; *Ndufa1*, *Ndufa2*. (B) CII; *Sdha*, *Sdhb*. (C) CIII; *Cyc1*, *Uqcrc1*. (D) CIV; *Cox4i1*, *Cox5a*, and ATPase (E); *Atp5a1*, *Atp5b*. Enzymatic activity of citrate synthase (F; CS, nM/min/mg) and  $\beta$ -hydroxyacyl-CoA dehydrogenase (G;  $\beta$ -HAD, nM/min/mg) in soleus muscles from WT and PyMT mice with or without 4 weeks of running exercise. A–E,  $n = 8$ –12 per group; F, G,  $n = 6$ –10 per group. Data presented as box-plot and whiskers-plot, median of the distribution is indicated as horizontal line, the boundaries indicate the medians of the first and third quartiles, and the error bars extend to the extremes of the observation. \* $P < 0.05$ , \*\* $P < 0.01$ , \*\*\* $P < 0.001$ .

PPAR $\gamma$  coactivator-1 $\alpha$  (PGC-1 $\alpha$ ) is an exercise-inducible transcriptional co-activator linked to mitochondrial numbers and volume, and improved exercise endurance in humans. PGC-1 $\alpha$  expression has been shown to be negatively regulated by TNF- $\alpha$  through NF- $\kappa$ B and p38 MAPK.<sup>29</sup> To evaluate the PGC-1 $\alpha$  response to exercise the gene expression was measured in muscle of WT and PyMT mice that had been running for 4 weeks (WT<sub>Ex</sub>, PyMT<sub>Ex</sub>) or inactive (WT, PyMT), as well as after all four groups had been challenged with a treadmill exhaustion run (Figure 2F and 2G). In line with our previous data and clinical studies,<sup>30,31</sup> PGC-1 $\alpha$  mRNA levels were not elevated after 4 weeks of chronic exercise training

(Figure 4N), but the level was increased in muscles after the treadmill run of exercised WT mice (WT<sub>Ex</sub>) as compared with non-exercised mice (WT). This treadmill-induced PGC-1 $\alpha$  response was not as evident in muscle from exercised PyMT mice (PyMT<sub>Ex</sub>), suggesting a tumour-induced dampening of PGC-1 $\alpha$  response and mitochondrial biogenesis (Figure 4O). Our results show that muscle from PyMT mice had lower expression of mitochondrial genes involved in the ETC, ATP production, and ROS scavenging, as well as lower mitochondrial enzyme activity (CS,  $\beta$ -HAD), but higher levels of intramuscular stress signals (TNF- $\alpha$ , p38 MAPK). The PGC-1 $\alpha$  response was blunted in PyMT as compared with WT mice, which pro-



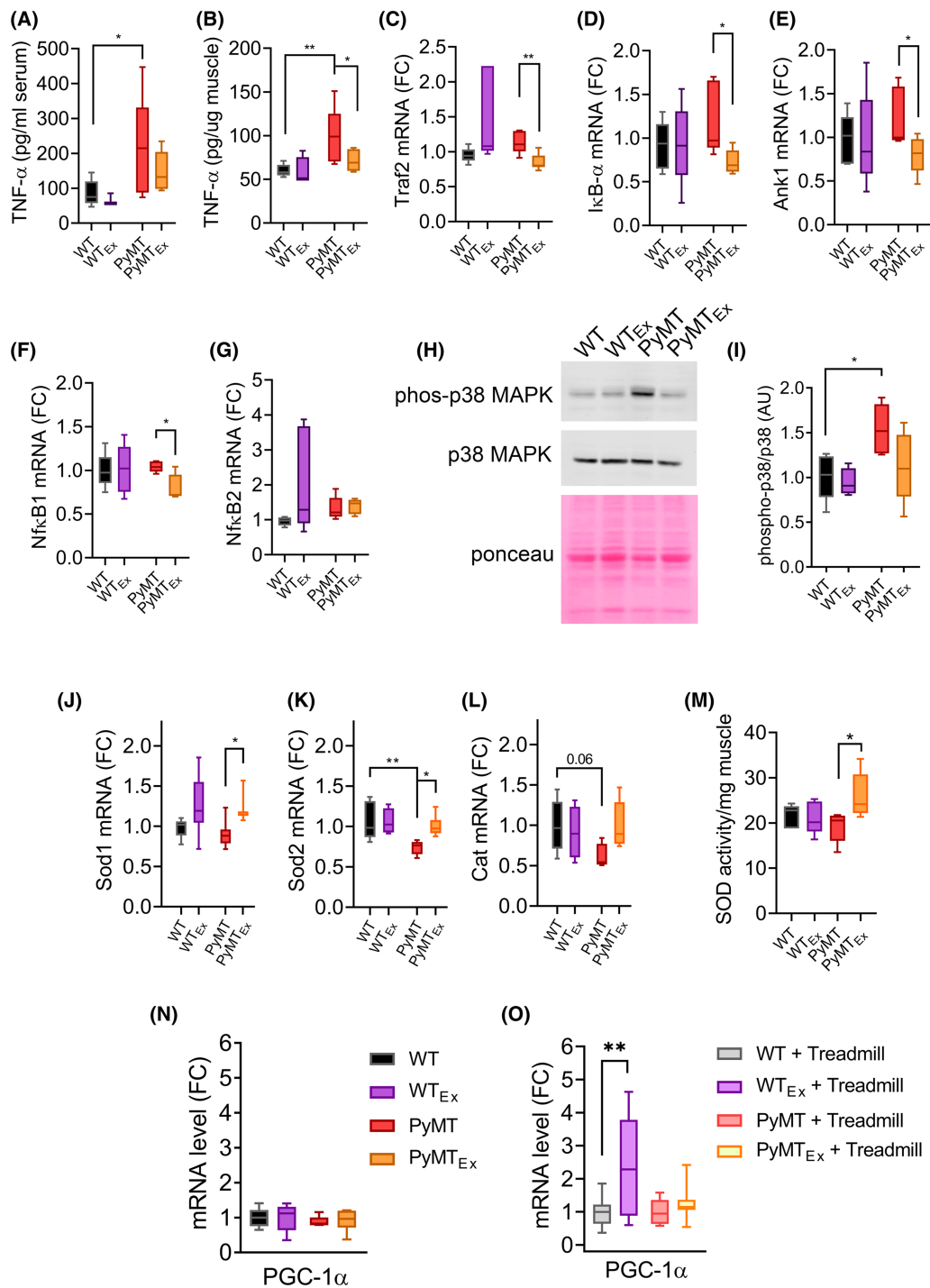


**Figure 4** Decreased intramuscular stress in PyMT mice after voluntary running. (A) TNF- $\alpha$  (pg/mL) in serum, (B) TNF- $\alpha$  (pg/ $\mu$ g) in soleus muscle homogenate and mRNA gene expression of TNF- $\alpha$  target genes (*Traf2*, *IkB- $\alpha$* , *Ank1*, *NfκB1*, *NfκB2*) (C–G) in gastrocnemius muscle from WT and PyMT mice after 4 weeks access to inactive (WT, PyMT) or active (WT<sub>Ex</sub>, PyMT<sub>Ex</sub>) in-cage running wheels. Representative immunoblots (H) and quantification (I) of phosphorylated and total p38 MAPK in TA muscle normalized to total protein (Ponceau S staining). (J–L) Antioxidant gene expression of SOD (*Sod1*, J; *Sod2*, K) and catalase (*Cat*) (L) and enzymatic activity of SOD (SO1 and SO2 combined) per mg of muscle (M) in gastrocnemius muscle from WT and PyMT mice after 4 weeks access to inactive (WT, PyMT) or active (WT<sub>Ex</sub>, PyMT<sub>Ex</sub>) in-cage running wheels. Gene expression of full-length PGC-1 $\alpha$  (N–O) in gastrocnemius muscle from WT mice after 4 weeks access to inactive or active in-cage running wheels (N) and after a treadmill exhaustion run after 4 weeks access to inactive or active in-cage running wheels (O) normalized to non-exercising mice (A–I, n = 6 per group; J–O, n = 8–12 per group;). Data presented as box-plot and whiskers-plot, median of the distribution is indicated as horizontal line, the boundaries indicate the medians of the first and third quartiles, and the error bars extend to the extremes of the observation. \*P < 0.05, \*\*P < 0.01.

vides a possible molecular link to mitochondrial gene expression and enzyme activities. Nevertheless, the exercise intervention was able to counteract the reduction in expression levels and enzyme activities, and reduce the intramuscular stress levels, resulting in improved force production and exercise performance in PyMT mice.

## Discussion

Loss of muscle mass is not a frequent complication in patients with breast cancer, but they still experience muscle weakness.<sup>3</sup> In agreement, we found no signs of muscle atrophy in 12-week-old PyMT mice, but they had reduced physical capacity as shown in a treadmill endurance test and exhibited muscle weakness according to force measurements. Here, the tumour-induced muscular dysfunction could be counteracted with 4 weeks of voluntary running. In addition, the exercise intervention induced beneficial molecular adaptations targeted at mitochondrial content and activity as well as systemic and intracellular stress relief, contributing to an overall improvement of muscle function in PyMT mice.

The muscle weakness was primarily observed in slow-twitch soleus muscle rather than fast-twitch extensor digitorum longus (EDL) muscle. Cancer-induced molecular changes in muscle of mixed fibre type (gastrocnemius, tibialis anterior) were also observed (e.g. ETC activity) but appeared more moderate compared with changes in slow-twitch soleus muscle. Thus, varied fibre type-specific differences were observed, which can have several underlying explanations. For instance, slow-twitch oxidative soleus fibres are recruited at a lower motor unit firing rate (~20 Hz) than fast-twitch glycolytic EDL fibres (~70 Hz),<sup>32</sup> and the twitch contraction time is longer in slow-twitch muscle fibres than fast-twitch fibres.<sup>28</sup> Thus, a higher number of slow-twitch fibres are activated during everyday movement and exercise at a moderate intensity, which demands a functional mitochondrial oxidative metabolism, whereas the glycolytic capacity of muscle is not challenged to the same extent. Our data show signs of decreased mitochondrial health in slow-twitch (and mixed) muscle type, which likely contributes to the observed alterations in oxidative slow-twitch, but not glycolytic fast-twitch muscles of PyMT mice. On the other hand, in tumour-bearing rodent models with a prominent muscle atrophy (bone cancer) slow-twitch muscle fibres appear more protected from cancer-induced muscle loss than fast-twitch muscle fibres.<sup>33</sup> Recent analyses of different muscles (soleus, EDL, gastrocnemius, etc.) displayed a high transcript diversity,<sup>34</sup> emphasizing the concept of skeletal muscle being a family of tissues with the commonality of contractile function but differences in physiology and metabolism. Thus, a muscle fibre type specific response to cancer-induced molecular and metabolic changes should be elucidated further

since it might influence the choice of therapeutic intervention to counteract cancer-induced muscle dysfunction.

Molecular pathways activated during breast cancer progression have been shown to overlap with intramuscular stress signals, for example, TNF- $\alpha$ , NF- $\kappa$ B. Exercise and physical activity are known to preserve muscle function through neutralizing intracellular stress, and promoting a healthier mitochondrial pool. Although exercise is thought to be beneficial breast cancer patients, the direct effects on cancer-related outcomes is poorly understood, partly because the effect of cancer itself versus anticancer treatment cannot be distinguished in clinical studies. Here, the PyMT mice did not receive anticancer treatment, and thus the exercise-induced effects presented here do not involve any treatment interference. Mice were placed on running wheels at 8 weeks of age when displaying palpable tumours. During the 4 weeks *ad libitum* running wheel access, WT and PyMT mice ran the same time and distance on the wheel, as previous reported.<sup>35</sup> Our exercise intervention improved the running capacity of both PyMT and WT mice, as they ran for a longer time and endured a longer distance during the treadmill exhaustion test which is an whole body performance indicator (Figure 2F and 2G), but the amplitude of improvement was lower in PyMT mice than healthy WT mice. Although the gain in running performance was lower in PyMT than in WT mice, it completely counteracted the muscle weakness observed in soleus muscle of PyMT mice. In addition to muscle weakness, cardiovascular disease (CVD) is a common co-morbidity in patients with cancer, including breast cancer,<sup>36,37</sup> with a 2–6 times higher CVD mortality risk than the general population.<sup>36</sup> Endurance exercise exerts beneficial effects on the whole body and can be used as a powerful tool to enhance cardiac and skeletal muscle function, subsequently reducing the mortality risk and enhancing the quality of life for patients with breast cancer.<sup>7</sup> In this study, the 4 weeks running and the subsequently improved running performance in the treadmill endurance test suggests favourable adaptations in both skeletal and cardiorespiratory health.

The PyMT mouse model is considered clinically relevant as it recapitulates human breast cancer progression *in vivo*.<sup>12,38</sup> The tumours of PyMT mice cluster with the luminal B subtype of human breast cancers, which accounts for nearly 40% of all breast cancers.<sup>39</sup> At the start of the voluntary wheel running (8-week-old mice), tumours are mostly in the adenoma stage with limited invasive properties into the surrounding tissue. At the experimental endpoint (12 weeks), most tumours are in an early carcinoma stage, with a higher degree of cytological atypia and begin of invasion of surrounding stroma.<sup>12</sup> The exercise started after tumour onset and thus mimics newly diagnosed breast cancer patients starting to exercise; therefore, this exercise intervention was not expected to have major effects on the tumour progression itself, as confirmed by our data. However, pathological markers in the tumour alternated towards a more favourable molecular tumour profile

after the exercise, that is, a slight increase of CK8 expression, indicates differentiation towards a normal luminal epithelial phenotype and the CK14 decrease shows halted tumour dedifferentiation towards a more aggressive phenotype.<sup>14</sup> Similarly, the same exercise intervention for 8 weeks from 4 weeks of age, did not alter tumour growth, but promoted a less tumorigenic microenvironment in PyMT mice.<sup>35</sup> Whereas voluntary running exercise for 10 weeks, starting at 6 weeks of age, showed an attenuation of tumour size in PyMT mice but had no significant effects on the tumour microenvironment.<sup>35,40</sup> Together, start date and duration of the exercise are important in establishing the effects on tumour growth and progression. Nevertheless, moderate exercise (mimicked here with voluntary running) is shown to be beneficial for patients with breast cancer, for example, 3–5 h of walking per week, post-diagnosis reduced breast cancer mortality risk with ~35%.<sup>7,41</sup>

Chronic and prolonged elevated levels of pro-inflammatory cytokines in plasma and/or intramuscularly, have detrimental effects on muscle function. In PyMT mice, a chronic stress state was indicated by higher levels of TNF- $\alpha$  and other cytokines in serum, higher intramuscular TNF- $\alpha$  levels and increased p38 MAPK stress response which is a known downstream target of TNF- $\alpha$ . Excess ROS contributes to oxidative stress and hence intramuscular stress. Mitochondria (primarily CI, CIII) and NADPH oxidases (NOX) 2 and 4 are known sources of ROS.<sup>28</sup> Here, muscle from PyMT mice had lower expression of CI-CIV and ATPase, and *Nox2* and

*Nox4* genes (Figure S2F and S2G) than WT controls. At the same time, no sign of global elevated oxidative stress levels in muscle from PyMT mice could be detected. This does not exclude local elevations of oxidative stress which could contribute to muscle dysfunction. Prolonged mitochondrial dysfunction can eventually also lead to ROS accumulation, but this could not be investigated here due to ethical restrictions regarding the experimental duration. For instance, reduced mitochondrial ETC content has been shown to result in elevated oxidative stress,<sup>42</sup> and hence, total content of mitochondria (and likely NOX) does not reflect its capacity to produce ROS.

Running exercise triggers mitochondrial biogenesis and the antioxidant defence system in skeletal muscle. The exercise intervention was able to normalize the intramuscular stress levels and downstream TNF- $\alpha$  target gene expression in PyMT mice to correspond to levels observed in that of WT mice. Running also revoked the expression of ETC and antioxidant genes, as well as CS,  $\beta$ -HAD and SOD enzyme activities. This shows that breast cancer imposes a stress condition on the skeletal muscle which can be mitigated with 4 weeks of voluntary running exercise. Furthermore, the acute exercise-induced PGC-1 $\alpha$  expression, and exercise-induced CS and  $\beta$ -HAD activity increases were blunted in muscle from the PyMT mice. This shows that breast cancer may interfere with skeletal muscle transcriptional programming of mitochondria and the molecular adaptation to exercise differs between healthy and breast cancer mice.

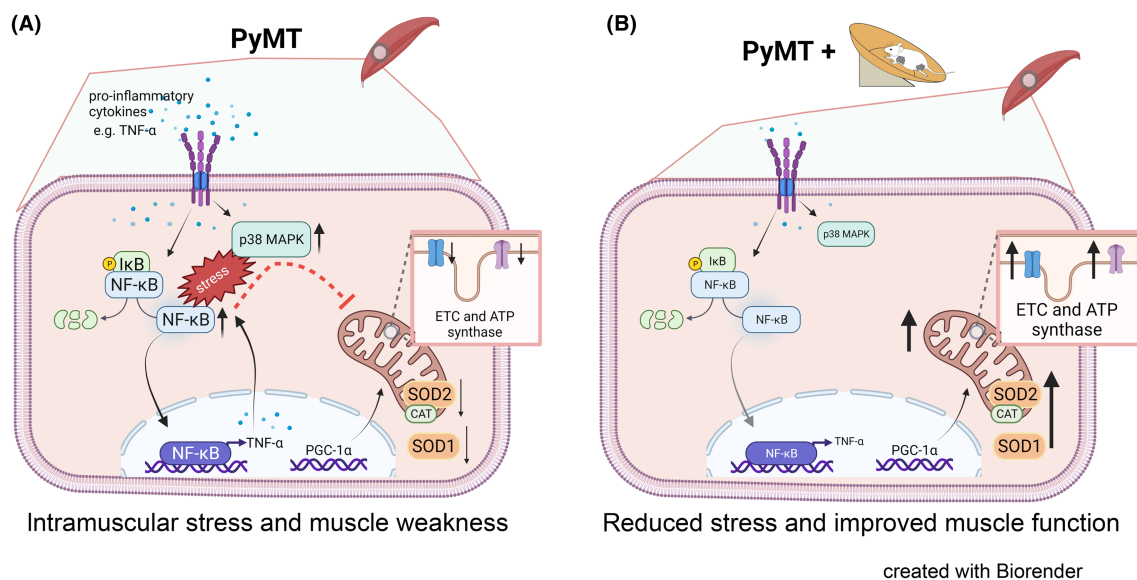


**Figure 5** Exercise in PyMT mice leads to a decrease in intramuscular stress-related pathways. Schematic illustration of our findings explaining underlying molecular mechanisms of muscle weakness in PyMT mice with breast cancer. (A) The breast cancer in PyMT mice leads to a reduced force production in skeletal muscle, caused by an increase in pro-inflammatory cytokines in the skeletal muscle, and hence activating intramuscular stress-related pathways via p38, TNF- $\alpha$  and NF- $\kappa$ B as well as decreasing ETC ( $P < 0.05$ ,  $P < 0.01$ ) and antioxidant genes. (B) Four weeks of in-cage voluntary running reduced the intramuscular stressors and the mitochondrial complex and antioxidant transcriptional profiles and enzyme activities increased to levels matching healthy WT controls. Together this contributed to that exercise counteracted the cancer-induced muscle weakness.

## Conclusions

Four-week voluntary wheel running was able to counteract the weakness in PyMT mice and resulted in reduced intrinsic stress and revoked mitochondrial and antioxidant gene expression and enzyme activities comparable with healthy WT levels. *Figure 5* summarizes the obtained results and the impact of exercise in PyMT mice. This adds novel insight into breast cancer-induced muscle weakness and molecular pathways that are involved in the beneficial effect of exercise on tumour-inflicted muscle.

## Acknowledgements

We thank Dr. Niklas Ivarsson, who left us too early, for his help with this study. This study was performed with the support from The Swedish Research Council (J. T. L., 2019-01282), Wenner–Gren Foundation (T. C., postdoc fellowship), Karolinska Institutet (T. M., doctorate funding). The histology

core facility at Biomedicum, Karolinska Institute supported the tissue processing for immunohistochemical analyses. E. w. K. and C. T. V. were supported by The Swedish Research Council (C. T. V., 2017-03056) and Swedish Cancer Society (C. T. V. and C. A. N., 2018/875). The authors of this manuscript certify that they comply with the ethical guidelines for authorship and publishing in the *Journal of Cachexia, Sarcopenia and Muscle*.<sup>43</sup>

## Online supplementary material

Additional supporting information may be found online in the Supporting Information section at the end of the article.

## Conflict of interest

The authors declare that they have no conflict of interest.

## References

- Westphal T, Gampenrieder SP, Rinnerthaler G, Greil R. Cure in metastatic breast cancer. *Memory* 2018;**11**:172–179.
- Freire PP, Fernandez GJ, Moraes D, Cury SS, Dal Pai-Silva M, Reis PP, et al. The expression landscape of cachexia-inducing factors in human cancers. *J Cachexia Sarcopenia Muscle* 2020;**11**:947–961.
- Baracos VE, Martin L, Korc M, Guttridge DC, Fearon KCH. Cancer-associated cachexia. *Nat Rev Dis Primers* 2018;**4**:17105.
- Christensen JF, Jones LW, Andersen JL, Daugaard G, Rorth M, Hojman P. Muscle dysfunction in cancer patients. *Ann Oncol* 2014;**25**:947–958.
- Klassen O, Schmidt ME, Ulrich CM, Schneeweiss A, Potthoff K, Steindorf K, et al. Muscle strength in breast cancer patients receiving different treatment regimens. *J Cachexia Sarcopenia Muscle* 2017;**8**:305–316.
- Kramer JA, Curran D, Piccart M, de Haes JCJM, Bruning P, Klijn J, et al. Identification and interpretation of clinical and quality of life prognostic factors for survival and response to treatment in first-line chemotherapy in advanced breast cancer. *Eur J Cancer* 2000;**36**:1498–1506.
- Lahart IM, Metsios GS, Nevill AM, Carmichael AR. Physical activity, risk of death and recurrence in breast cancer survivors: A systematic review and meta-analysis of epidemiological studies. *Acta Oncol* 2015;**54**:635–654.
- Ibrahim EM, Al-Homaidh A. Physical activity and survival after breast cancer diagnosis: meta-analysis of published studies. *Med Oncol* 2011;**28**:753–765.
- Ammitzbøll G, Sjøgaard K, Karlsen RV, Tjønneland A, Johansen C, Frederiksen K, et al. Physical activity and survival in breast cancer. *Eur J Cancer* 2016;**66**:67–74.
- Holick CN, Newcomb PA, Trentham-Dietz A, Titus-Ernstoff L, Bersch AJ, Stampfer MJ, et al. Physical activity and survival after diagnosis of invasive breast cancer. *Cancer Epidemiol Biomarkers Prev* 2008;**17**:379–386.
- Mijwel S, Cardinale DA, Norrbom J, Chapman M, Ivarsson N, Wengström Y, et al. Exercise training during chemotherapy preserves skeletal muscle fiber area, capillarization, and mitochondrial content in patients with breast cancer. *FASEB J* 2018;**32**:5495–5505.
- Lin EY, Jones JG, Li P, Zhu L, Whitney KD, Muller WJ, et al. Progression to malignancy in the polyoma middle T oncoprotein mouse breast cancer model provides a reliable model for human diseases. *Am J Pathol* 2003;**163**:2113–2126.
- Liu Z, Chaillou T, Santos Alves E, Mader T, Jude B, Ferreira DMS, et al. Mitochondrial NDUFA4L2 is a novel regulator of skeletal muscle mass and force. *FASEB J* 2021;**35**:e22010, <https://doi.org/10.1096/fj.202100066R>
- Cheung KJ, Gabrielson E, Werb Z, Ewald AJ. Collective invasion in breast cancer requires a conserved basal epithelial program. *Cell* 2013;**155**:1639–1651.
- Chaillou T, McPeck A, Lanner JT. Docetaxel does not impair skeletal muscle force production in a murine model of cancer chemotherapy. *Physiol Rep* 2017;**5**:e13261, <https://doi.org/10.14814/phy2.13261>
- Cheng AJ, Westerblad H. Mechanical isolation, and measurement of force and myoplasmic free [Ca<sup>2+</sup>] in fully intact single skeletal muscle fibers. *Nat Protoc* 2017;**12**:1763–1776.
- Lanner JT, Georgiou DK, Joshi AD, Hamilton SL. Ryanodine receptors: structure, expression, molecular details, and function in calcium release. *Cold Spring Harb Perspect Biol* 2010;**2**:a003996, <https://doi.org/10.1101/cshperspect.a003996>
- Bass A, Brdiczka D, Eyer P, Hofer S, Pette D. Metabolic differentiation of distinct muscle types at the level of enzymatic organization. *Eur J Biochem* 1969;**10**:198–206.
- Allen DG, Westerblad H. The effects of caffeine on intracellular calcium, force and the rate of relaxation of mouse skeletal muscle. *J Physiol* 1995;**487** (Pt 2):331–342.
- Owen AM, Patel SP, Smith JD, Balasuriya BK, Mori SF, Hawk GS, et al. Chronic muscle weakness and mitochondrial dysfunction in the absence of sustained atrophy in a pre-clinical sepsis model. *Elife* 2019;**8**:8.
- Migliavacca E, Tay SKH, Patel HP, Sonntag T, Civiletto G, McFarlane C, et al. Mitochondrial oxidative capacity and NAD(+) biosynthesis are reduced in human sarcopenia across ethnicities. *Nat Commun* 2019;**10**:5808.
- Wilson HE, Stanton DA, Montgomery C, Infante AM, Taylor M, Hazard-Jenkins H, et al. Skeletal muscle reprogramming by breast cancer regardless of treatment history or tumor molecular subtype. *NPJ Breast Cancer* 2020;**6**:18.

23. Vigelsø A, Andersen NB, Dela F. The relationship between skeletal muscle mitochondrial citrate synthase activity and whole body oxygen uptake adaptations in response to exercise training. *Int J Physiol Pathophysiol Pharmacol* 2014;**6**:84–101.
24. Mercogliano MF, Bruni S, Elizalde PV, Schillaci R. Tumor Necrosis Factor  $\alpha$  Blockade: An Opportunity to Tackle Breast Cancer. *Front Oncol* 2020;**10**:584.
25. Stasko SA, Hardin BJ, Smith JD, Moylan JS, Reid MB. TNF signals via neuronal-type nitric oxide synthase and reactive oxygen species to depress specific force of skeletal muscle. *J Appl Physiol* (Bethesda, Md: 1985), 2013;**114**(11):1629–1636.
26. Nisr RB, Shah DS, Ganley IG, Hundal HS. Proinflammatory Nf $\kappa$ B signalling promotes mitochondrial dysfunction in skeletal muscle in response to cellular fuel overloading. *Cell Mol Life Sci* 2019;**76**:4887–4904.
27. Hardin BJ, Campbell KS, Smith JD, Arbogast S, Smith J, Moylan JS, et al. TNF- $\alpha$  acts via TNFR1 and muscle-derived oxidants to depress myofibrillar force in murine skeletal muscle. *J Appl Physiol* (1985) 2008;**104**:694–699.
28. Cheng AJ, Yamada T, Rassier DE, Andersson DC, Westerblad H, Lanner JT. Reactive oxygen/nitrogen species and contractile function in skeletal muscle during fatigue and recovery. *J Physiol* 2016;**594**:5149–5160.
29. Palomer X, Álvarez-Guardia D, Rodríguez-Calvo R, Coll T, Laguna JC, Davidson MM, et al. TNF- $\alpha$  reduces PGC-1 $\alpha$  expression through NF- $\kappa$ B and p38 MAPK leading to increased glucose oxidation in a human cardiac cell model. *Cardiovasc Res* 2009;**81**:703–712.
30. Ivarsson N, Mattsson CM, Cheng AJ, Bruton JD, Ekblom B, Lanner JT, et al. SR Ca(2+) leak in skeletal muscle fibers acts as an intracellular signal to increase fatigue resistance. *J Gen Physiol* 2019;**151**:567–577.
31. Norheim F, Langleite TM, Hjorth M, Holen T, Kielland A, Stadheim HK, et al. The effects of acute and chronic exercise on PGC-1 $\alpha$ , irisin and browning of subcutaneous adipose tissue in humans. *FEBS J* 2014;**281**:739–749.
32. Schiaffino S, Reggiani C. Fiber types in mammalian skeletal muscles. *Physiol Rev* 2011;**91**:1447–1531.
33. Alves CRR, Eichelberger EJ, das Neves W, Ribeiro MAC, Bechara LRG, Voltarelli VA, et al. Cancer-induced muscle atrophy is determined by intrinsic muscle oxidative capacity. *FASEB J* 2021;**35**:e21714, <https://doi.org/10.1096/fj.202100263R>
34. Terry EE, Zhang X, Hoffmann C, Hughes LD, Lewis SA, Li J, et al. Transcriptional profiling reveals extraordinary diversity among skeletal muscle tissues. *Elife* 2018;**7**:e34613, <https://doi.org/10.7554/eLife.34613>
35. Rundqvist H, Veliça P, Barbieri L, Gameiro PA, Bargiela D, Gojkovic M, et al. Cytotoxic T-cells mediate exercise-induced reductions in tumor growth. *Elife* 2020;**9**:9.
36. Sturgeon KM, Deng L, Bluethmann SM, Zhou S, Trifiletti DM, Jiang C, et al. A population-based study of cardiovascular disease mortality risk in US cancer patients. *Eur Heart J* 2019;**40**:3889–3897.
37. Maayah ZH, Takahara S, Alam AS, Ferdaoussi M, Sutendra G, el-Kadi AOS, et al. Breast cancer diagnosis is associated with relative left ventricular hypertrophy and elevated endothelin-1 signaling. *BMC Cancer* 2020;**20**:751.
38. Attalla S, Taifour T, Bui T, Muller W. Insights from transgenic mouse models of PyMT-induced breast cancer: recapitulating human breast cancer progression in vivo. *Oncogene* 2021;**40**:475–491.
39. Li Z-H, Hu PH, Tu JH, Yu NS. Luminal B breast cancer: patterns of recurrence and clinical outcome. *Oncotarget* 2016;**7**:65024–65033.
40. Goh J, Tsai J, Bammler TK, Farin FM, Endicott E, Ladiges WC. Exercise training in transgenic mice is associated with attenuation of early breast cancer growth in a dose-dependent manner. *PLoS One* 2013;**8**:e80123, <https://doi.org/10.1371/journal.pone.0080123>
41. Holmes MD, Chen WY, Feskanich D, Kroenke CH, Colditz GA. Physical activity and survival after breast cancer diagnosis. *JAMA* 2005;**293**:2479–2486.
42. Jang YC, Lustgarten MS, Liu Y, Muller FL, Bhattacharya A, Liang H, et al. Increased superoxide in vivo accelerates age-associated muscle atrophy through mitochondrial dysfunction and neuromuscular junction degeneration. *FASEB J* 2010;**24**:1376–1390.
43. von Haehling S, Morley JE, Coats AJS, Anker SD. Ethical guidelines for publishing in the Journal of Cachexia, Sarcopenia and Muscle: update 2021. *J Cachexia Sarcopenia Muscle* 2021;**12**:2259–2261.